JOURNAL OF MATERIALS SCIENCE 7 (1972) 23–30

Some Observations on the Deformation Characteristics of Titanium Hydride

P. E. IRVING, C. J. BEEVERS
Department of Physical, Metallurgy and Science of Materials, University of Birmingham, UK

Deformation studies have been performed on bulk polycrystalline titanium hydride, of compositions between $TiH_{1.53}$ and $TiH_{1.99}$, and at temperatures between − 35 and 200° C. The yield stress increased with decreasing temperature and with increasing non-stoichiometric hydrogen vacancy content. The temperature dependence of the yield stress was enhanced with increasing vacancy content. Two-surface analysis of slip lines revealed that the slip plane was {111}. Strain-rate tests on $TiH_{1.65}$ demonstrated a considerable strain-rate dependence of both yield and fracture characteristics. The effects of test temperature, non-stoichiometric defect concentration and strain-rate on the deformation and fracture characteristics are shown to be strongly related to hydrogen ion mobility.

1. Introduction

Group IIIA, IVA and VA transition metals can all combine with hydrogen to form a series of pseudo-metallic hydrides. In general these compounds are non-stoichiometric, and their atomic bonding is thought to be partially ionic and partially metallic in nature [1]. This paper will be concerned with titanium hydride, whose characteristics are closely allied to hydrides of the other two metals in group IVA, namely zirconium and hafnium.

Titanium hydride has a fluorite structure [1] with metal atoms on an fcc lattice and hydrogen atoms in the tetrahedral interstices. Consequently the maximum hydrogen to metal ratio is two. Non-stoichiometry is accommodated by hydrogen vacancies [2] and the single phase hydride of lowest hydrogen content is of composition $TiH_{1.59}$ [3]. At hydrogen contents greater than $TiH_{1.90}$ the c-axis of the unit cell contracts, and the resulting tetragonal hydride has $c/a \approx 0.98$ [3]. The tetragonal transformation is thought to be similar to the diffusionless twinning mechanism known to operate in the cubic/tetragonal transformation in zirconium hydride [4]. Above 40° C, tetragonal titanium hydride reverts to the cubic form [5].

The mechanical properties and deformation mechanisms of other compounds having fluorite structures have been studied [6-8]. Roy [6], working with single crystals of fluorite, showed that the slip planes were {100}, with {110} operating at temperatures above 200° C, the slip direction in both cases being ⟨110⟩. Similar results have been obtained for UO_2 [7] and ThO_2 [8] but in these compounds, the {111} slip plane was operative at elevated temperatures when ionic bonding had been relaxed.

The mechanical properties of zirconium hydrides have been studied by Mueller [9] and Barraclough [10, 11]. Using compression tests on polycrystalline material, Barraclough showed that the single-phase cubic hydride was brittle below 100° C. Above this temperature, glide on {111} planes enabled polycrystalline ductility to be achieved. The yield stress showed a marked decrease with temperature from 100 to 200° C, but was relatively temperature insensitive above 200° C. Similar behaviour was noted for tetragonal hydrides except that they were less temperature dependent, and deformed to a substantial degree by a process of stress-induced twin boundary interface motion [11].

No assessment could be made of the influence of non-stoichiometry on the yield stress in zirconium hydride, owing to the limited extent of the single-phase field. Titanium hydride has, on the other hand, a wide non-stoichiometric range, and it was with the object of investigating this and other factors affecting mechanical behaviour, that work was initiated into the compressive strengths of this material.

2. Experimental

2.1. Starting Materials and Hydride Preparation

Iodide titanium was arc-melted and hot-rolled under argon to sheet 3 mm thick. Bars 3 mm wide were cut from this and electropolished in a solution of 95 vol % glacial acetic acid, 5 vol % perchloric acid and an e.m.f. of 30 volts. Analysis of the bars revealed about 300 ppm atomic impurity.

Bulk pseudo-metallic hydrides can be manufactured by a direct gas-metal reaction as carried out by Barraclough when preparing zirconium hydride [12]. In the present case, a similar method was used, the details of which are available from [13]. The titanium bars were initially heated to 900°C under a vacuum of 10^{-5} torr. Hydrogen was introduced into the system whilst at this temperature, and will dissolve in the β-phase titanium directly, forming a solid solution. Subsequent control of cooling-rates and hydrogen pressures enabled individual specimens of hydride to be manufactured to a desired hydrogen content. Extremely slow cooling rates ($\sim$ 50°C/day) were necessary to avoid specimen cracking during the transformation to hydride, and up to 3 to 4 weeks were required to prepare a single composition. Weight measurements before and after hydriding were used to determine the composition of the resulting hydride. Analysis of the hydride bars showed that they contained $\sim$ 1000 ppm atomic impurity, mostly oxygen (500 ppm) and carbon (250 ppm). Consequently the error in determining a hydride composition of TiH_x would be $x \pm 0.01$.

2.2. Preparation and Testing of Compression Specimens

After hydriding, surface layers of the bars were generally cracked, and the bars themselves slightly warped. To eliminate these defects, 0.5 mm was removed from each of the four bar faces using a diamond saw. The remaining bar then contained lengths of crack-free hydride trimmed to a square cross-section. These were electropolished using a 95 vol % glacial acetic acid, 5 vol % perchloric acid solution and an e.m.f. of 18 to 22 volts. The lower the hydrogen content of the hydride the higher the e.m.f. required to polish. Compression specimens 3 mm long were then cut out of the polished bars, again using the diamond saw.

When testing in compression, a height-to-diameter ratio of 3.0 is desirable as the best compromise between barrelling and buckling tendencies occurring at lower and higher h/d ratios respectively. An h/d ratio of 1.5 was chosen to enable more specimens to be cut from a single bar. Decreasing the h/d ratio from the value of 3.0 causes the observed macroscopic yield stress to increase, but this effect is negligible for h/d ratios greater than unity [14].

The above method of preparation was used to produce compression specimens of $TiH_{1.53}$, $TiH_{1.58}$, $TiH_{1.63}$, $TiH_{1.65}$, $TiH_{1.67}$, $TiH_{1.75}$, $TiH_{1.80}$, $TiH_{1.91}$, and $TiH_{1.99}$. Metallographic and X-ray powder pattern examination revealed that all hydrides except $TiH_{1.53}$, $TiH_{1.58}$ and $TiH_{1.91}$ were single phase and cubic. $TiH_{1.58}$ had a small quantity of Widmanstätten α-titanium precipitate; $TiH_{1.53}$ an increased proportion. $TiH_{1.91}$ was partially transformed to the tetragonal phase, but will revert to the cubic form above 40°C [5]. Grain sizes of all hydride specimens varied between an average for each composition of 0.04 to 0.06 mm across, there being wide variation in individual grain size.

Mechanical tests were performed in a compression jig fitted to a hard-beam tensile machine, using a strain rate of 9.0×10^{-4} sec^{-1}. Strain-rate tests were performed on $TiH_{1.65}$ using the same compression jig and an Instron testing facility at strain rates between 1.88×10^{-4} and 1.88×10^{-1} sec^{-1}.

Tests above room temperature were conducted in a heated silicone oil bath, tests below room temperature in baths of ice and water, or acetone cooled with liquid nitrogen.

3. Results

At room temperature and above, all hydride specimens with the exception of $TiH_{1.99}$ were able to accommodate some plastic strain. $TiH_{1.99}$ fractured without detectable plastic strain at 0°C, and at 24°C, and only accommodated 0.5% strain at 108°C. Other hydride specimens did not exhibit such brittle behaviour until temperatures below 0°C were attained. Fig. 1 shows the yield or fracture stress of all the tested compositions plotted as a function of temperature. In general the yield or fracture stress decreases with increasing temperature, but the curves become more temperature-dependent as the vacancy concentration increases. Increasing the non-stoichiometric vacancy content also increases the hydride yield or fracture stress.

All hydrides which accommodated any plastic strain underwent a smooth elastic/plastic transi-

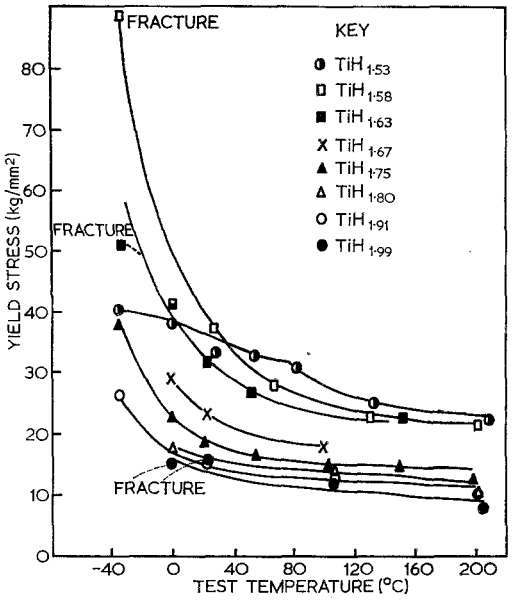

Figure 1 Hydride yield or fracture stresses plotted as a function of temperature.

tion; examples of the stress-strain curves obtained are shown in fig. 2, for specimens of $TiH_{1.75}$.

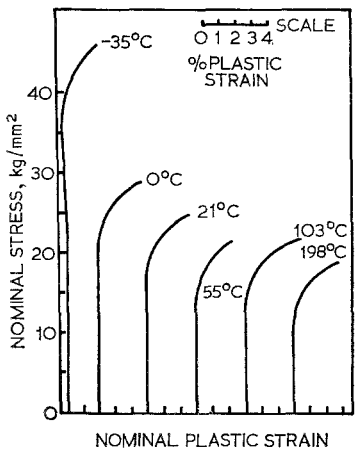

Figure 2 Typical stress-strain curves of $TiH_{1.75}$.

Fracture stresses increase with increasing non-stoichiometric defect in a systematic manner, echoing the yield stress behaviour found at higher temperatures. Consequently it is thought that fracture stresses reflect the anticipated yield behaviour of hydrides tested at low temperatures.

Slip lines were readily observed on the surface of all specimens accommodating plastic strain

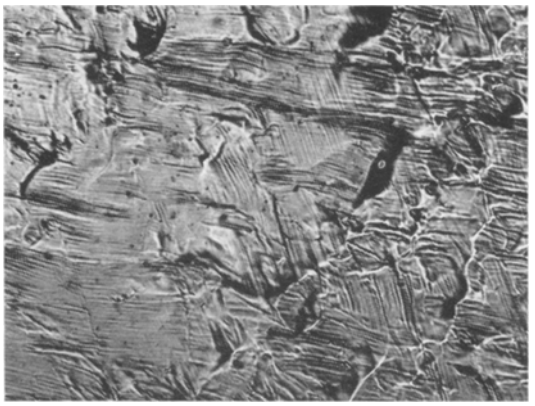

Figure 3 Slip lines on $TiH_{1.75}$ deformed 15% at 150°C (× 250).

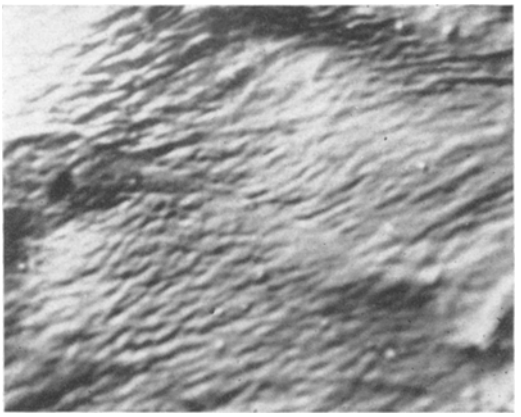

Figure 4 Slip lines on $TiH_{1.75}$ deformed 2% at − 35°C (× 650).

(figs. 3 and 4). These tended to become finer and less straight as the test temperature was lowered. $TiH_{1.75}$ which accommodated 2% strain at − 35°C, had localised portions of its surface covered in wavy slip lines (fig. 4). As the non-stoichiometric vacancy concentration increased, and the temperature decreased, slip became a more localised phenomenon, and was generally accompanied by microcrack formation after only 2 to 3% strain. In comparison, specimens of $TiH_{1.80}$ and $TiH_{1.91}$ could be strained 15 to 20% at 150 to 200°C without surface cracking.

Back reflection Laue patterns were taken of corner grains in deformed specimens of $TiH_{1.75}$, $TiH_{1.67}$, $TiH_{1.63}$ and $TiH_{1.58}$, and by means of two surface analysis, the slip planes were found to be {111}. Similar analyses could not be

performed on other hydride compositions as there was a lack of suitable corner grains. Similarly, analysis of microcrack directions enabled the cleavage planes to be deduced to be {111}, {110} and {100}, the {111} plane predominating in 50% of the analyses. The {111} cleavage plane is in agreement with that found by Roy [6] in single crystals of fluorite and with the observations of Libowitz and Pack [15] on cleaving single crystals of cerium dihydride, which also has a fluorite structure.

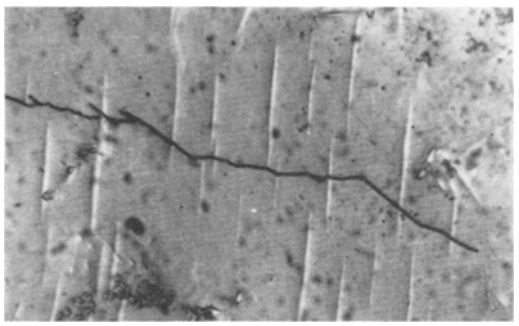

Figure 5 Crack propagating through titanium platelets in $TiH_{1.53}$ strained 3% at 30° C (× 680).

The presence of titanium precipitates in $TiH_{1.58}$ did not seem to influence the deformation behaviour of this hydride. However this was not the case with $TiH_{1.53}$. The mechanical behaviour of $TiH_{1.53}$ at temperatures below 83°C was radically different from the other hydrides. There was no prominent rise in the yield stress at low temperatures; specimens of this composition yielded at 30 to 40 kg/mm² (fig. 1). After yield, a high nominal work-hardening rate occurred, fracture occurring after less than 1% strain below room temperature. At room temperature and above, the hydride could be strained 1 to 2% without fracture, but was badly cracked (fig. 5). Specimens of $TiH_{1.53}$ tested above 83°C were similar to other hydrides in their deformation behaviour. It is thought that in these tests the hydride was single-phase. Below 83°C the hydride is thought to be two-phase. Differences in the elastic moduli, and stresses around the precipitates induced by the density change from hydride to titanium will cause crack-initiation in the hydride matrix on testing. As can be seen from fig. 5, titanium precipitates can cause propagating cracks to change direction, presumably absorbing energy as they cross them, and hence it will be possible for a period of relatively stable crack growth to occur, prior to final fracture. This will enable some strain to be accommodated, and much of the strain in low temperature tests of $TiH_{1.53}$ is thought to be due to this mechanism.

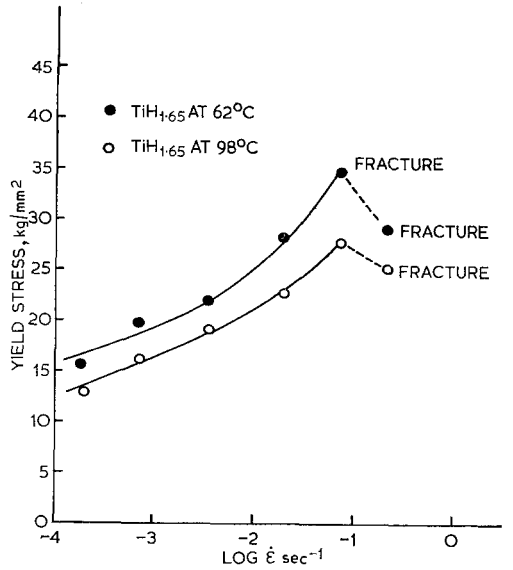

Figure 6 Yield and fracture stresses of $TiH_{1.65}$ plotted against strain-rate.

Strain-rate tests were performed with $TiH_{1.65}$. Six specimens each were tested at 62°C and at 98°C. Yield or fracture stresses plotted against applied strain rate are shown in fig. 6. It will be seen that there is a considerable dependence of the yield or fracture stress on the strain rate, both of these increasing with strain rate. Exceptions are the two specimens tested at the highest rate of strain. The dependence of the specimens tested at 98°C is slightly less than those tested at 62°C; a change in strain rate of 400× producing a 210% increase of the yield stress in the former case, and 230% in the latter. In addition, the specimens tested at 98°C could be subjected to a greater rate of strain before brittle fracture occurred, than could the ones tested at 62°C.

Examination of specimen surfaces after testing revealed that at both test temperatures slip lines became wavy as the brittle region was neared (figs. 7 and 8).

Instantaneous changes in the strain rate after yield were made during testing of these specimens, and from the incremental changes in stress, an estimate of the activation volume was made.

Figure 7 Slip lines on $TiH_{1.65}$ strained 2% at 62° C at strain-rate of 1.88×10^{-4} (× 520).

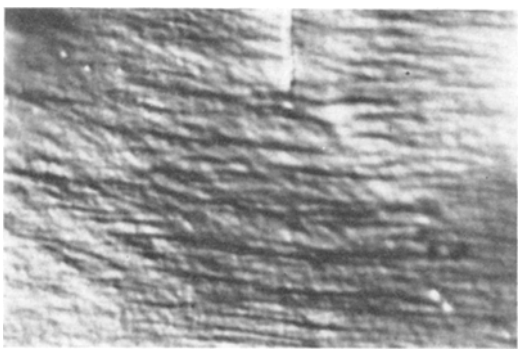

Figure 8 Slip lines on $TiH_{1.65}$ strained at 1.5% at 62° C at strain-rate of 1.88×10^{-2} (× 400).

Assuming the resolved shear stress was between one half and one tenth of the polycrystalline macroscopic yield stress, the activation volume can be calculated to be between $70b^3$ and $350b^3$.

4. Discussion

4.1. Slip and the Role of Hydrogen Diffusion

The observation of a {1 1 1} slip plane in titanium hydride is in accord with the conclusions of Barraclough [10] as to the slip plane in zirconium hydride. When considered in conjunction with the findings of an electron-microscopic investigation [13], that the slip-dislocation Burgers vectors are likely to be ⟨1 1 0⟩, it will be seen that there are twelve possible slip systems, This is ample to satisfy the von Mises criterion of five independent slip systems for polycrystalline ductility, and is as would be expected if the hydride consisted of an fcc metal lattice alone. However, it has been pointed out by Roy [6] that slip on a {1 1 1} ⟨1 1 0⟩ system in the fluorite lattice will involve electrostatic faulting of the ions in the tetrahedral lattice sites (in this case the hydrogen ions) and that there will be strong forces opposing dislocation motion on such a slip plane. It must be concluded either that the component of electrostatic bonding in group IVA metal hydrides is not significant, running counter to current thinking on the subject [1, 16], or that hydrogen ions avoid being faulted as a dislocation line passes on a {1 1 1} plane. Clearly, hydrogen ion diffusion would facilitate dislocation motion if the latter were the case, and a correlation should exist between hydrogen diffusion rates and the observed macroscopic yield stresses.

Stalinski [17] has investigated hydrogen mobilities in titanium hydride, and obtains an activation energy for hydrogen diffusion which is dependent on the hydrogen content of the hydride, varying between 9.5 and 10.5 kcal/mole. Using NMR techniques, Stalinski observed that a rigid hydrogen lattice existed at temperatures below about 0°C for hydrides of compositions below $\approx TiH_{1.90}$, the temperature at which the lattice began to break up increasing slightly with increasing hydrogen content.

Stalinski's results can be represented by an equation of the usual Arrhenius form:

$$V_c = V_0 n \left(\frac{d}{2}\right) \exp\left(\frac{-E_a}{RT}\right) \qquad (1)$$

Where V_c is the hydrogen jump frequency,
V_0 is a frequency factor,
n is the number of tetrahedral sites into which a hydrogen ion can jump,
d is the non-stoichiometric defect in the hydride, representing the probability that a hydrogen site is vacant,
E_a is the activation energy for hydrogen diffusion,
R is the gas constant,
T is the absolute temperature.

However, from Stalinski's results, both E_a and V_0 depend on d and E_a can be replaced by

$$\left(10.5 - \frac{d}{0.4}\right)$$

and V_0 by

$$V_0^0 \left(1.80 - \frac{d}{0.28}\right)$$

and the equation is modified to the form:

$$V_c = n\left(\frac{d}{2}\right) V_0^0 \left(1.80 - \frac{d}{0.28}\right) \exp\left(\frac{-1}{RT}\left(10.5 - \frac{d}{0.4}\right)\right) \quad (2)$$

Stalinski assumes a diffusion path along ⟨111⟩ between tetrahedral sites, hence $n = 4$ and he concludes that $V_0^0 \approx 10^{12}$.

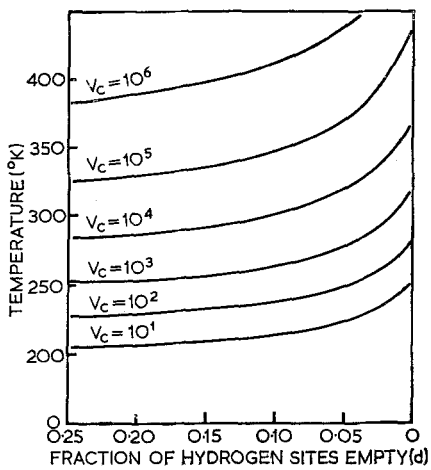

Figure 9 Graphs showing the interrelationship of V_c, T and d.

The values of V_c obtained from this equation will not be absolute ones, as the constants are not known with sufficient accuracy, but this does not invalidate the general form and application of the equation. Inserting values of T and d into equation (2), values of V_c can be plotted as in fig. 9. It will be seen that the temperature required to attain a given value of V_c varies little over most of the non-stoichiometric range, but at defect concentrations less than 0.05, it increases rapidly. If hydrogen ion mobility is a controlling factor in hydride deformation, then from fig. 9, a marked difference in the mechanical properties of $TiH_{1.99}$ when compared with the other tested compositions, can be expected. Indeed, $TiH_{1.99}$ was brittle at room temperature and below, and could only be strained 0.5% at 108°C. This can be compared with, for example, the strains of 12 to 15% accommodated without fracture by $TiH_{1.91}$ and $TiH_{1.75}$ when tested at these temperatures.

The significance of hydrogen ion mobility is further demonstrated in fig. 10, where hydride yield or fracture stresses are plotted as a function of hydrogen jump frequency calculated for each

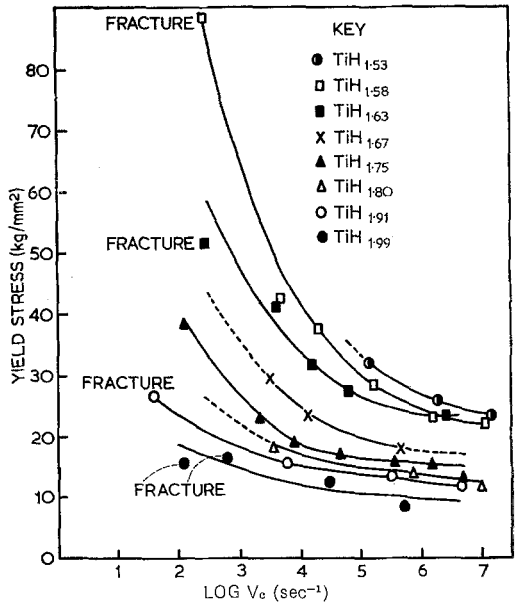

Figure 10 Yield or fracture stress plotted as a function of hydrogen jump frequency.

test from a knowledge of T and d. The curves obtained are similar to those obtained by plotting yield stress against temperature, but the curves of hydrides with high hydrogen content are shifted with respect to the others, to lower jump frequencies. It is clear from fig. 10 that all hydride compositions which fractured without detectable plastic strain were tested at temperatures which produced a value of the hydrogen jump frequency below 10^3/sec. The absolute value of this constant will be affected by the constants in equation (2), by the fact that polycrystalline material was used, and by the applied strain rate. However, for a strain rate of 9.0×10^{-4} sec^{-1}, for the particular grain size and equation constants used, the value is 10^3 sec^{-1}. This behaviour can be explained by postulating that in this region hydrogen mobilities were insufficient to prevent ion-ion interactions during slip on {111} planes, and consequently, the preferred slip plane will be the more usual {100}. As {100} ⟨011⟩ has insufficient slip variants for polycrystalline ductility, fracture will occur without detectable plastic strain [18]. In polycrystalline material, there will exist a transition region, where owing to the varied orientation of the grains, both {111} and {100} slip could be activated with a common slip direction. Such behaviour is thought to account for the wavy slip observed in fig. 4.

It is perhaps surprising that such good agreement with hydrogen mobility was obtained, when no account was taken of the fact that the atomic re-arrangements involved will be occurring at the dislocation core and bulk diffusion data will not apply. However, some form of Arrhenius Equation will still be valid, the terms in equation (2) affected at the core being the value of n and the maximum values of E_a and V_0. For the situation existing at the dislocation core, all these can be treated as constants and considered together with the others affecting the absolute values of V_c. The variables affecting the relative values of V_c for hydrides of different compositions, namely d and T, are unaffected.

The value of hydrogen jump frequency at which ion-ion interactions occur is clearly related to dislocation velocity, and in turn, will be related to the applied strain rate. This suggests that the jump frequency below which brittle behaviour is initiated will be dependent on the applied strain rate. From fig. 6 it will be seen that $TiH_{1.65}$ tested at 62°C, having a jump frequency of $\approx 10^5\ sec^{-1}$ became brittle at strain-rates between 1.88×10^{-2} and $7.48 \times 10^{-2}\ sec^{-1}$. During testing at 98°C, and a jump frequency of $\approx 5 \times 10^5\ sec^{-1}$, brittle behaviour commenced between the strain-rates of $7.48 \times 10^{-2}\ sec^{-1}$ and $1.88 \times 10^{-1}\ sec^{-1}$. When tested at a strain-rate of $9.0 \times 10^{-4}\ sec^{-1}$ hydrides of all compositions behaved in a brittle manner at jump frequencies below $10^3\ sec^{-1}$. In conclusion, an increase in jump frequency by factors of 100 and 500, necessitated an increase of strain-rate by factors of 80 and 200 before brittle behaviour could again be obtained. This must be regarded as a qualitative correlation, as the conditions for the onset of brittle behaviour have not been precisely determined. The fact that the material is polycrystalline will introduce a further unknown error into the analysis, but the combined effect of strain-rate and jump frequency on hydride mechanical behaviour can be seen. Further evidence that jump frequency and strain-rate act together to determine deformation behaviour is provided by the occurrence of wavy slip lines at 62 and 98°C when testing at high strain-rates. They would be formed by a similar mechanism to that outlined above for the occurrence of this type of slip at lower strain-rates at − 35°C.

The occurrence of additional slip planes in a material under deformation usually results in increased ductility [19]; in this case however, the two planes would only be operative together over a limited temperature range prior to the {111} becoming inoperative, the remaining {100} being insufficient for polycrystalline ductility.

4.2. The Role of Lattice Vacancies

In view of the observed dependence of hydride mechanical behaviour on hydrogen mobility, the dramatic effect of non-stoichiometric hydrogen vacancies is difficult to understand. At high jump frequencies they cause the yield stress to be doubled (as d is increased from 0.005 to 0.200), at low jump frequencies, they cause the yield or fracture stress to be increased some five times over the same non-stoichiometric range (fig. 10). The effect can be seen more clearly if points are interpolated from fig. 10 at constant values of V_c, and replotted as yield stress versus defect concentration (fig. 11).

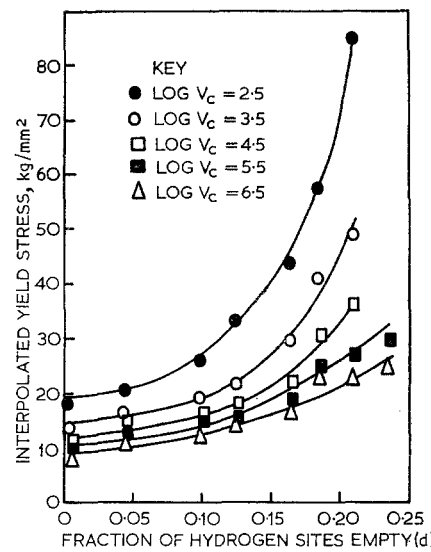

Figure 11 Yield or fracture stress plotted as a function of d at constant values of V_c. Points interpolated from fig. 10.

From figs. 10 and 11 it will be seen that the vacancy-hardening effect, in addition to the transition to brittle behaviour, can be correlated with hydrogen mobility. Tests demonstrating a pronounced dependence of the yield stress on strain-rate (fig. 6) confirm this view. However, the hardening cannot be due to the interaction of single vacancies and dislocations, as these will tend to decrease the probability of ion-ion interactions and have the reverse of the observed

effect. Hydrogen ion mobility *per se*, whether initiated by increased temperature and/or increased vacancy concentration has relatively little effect on yield stress, as can be seen from the behaviour of $TiH_{1.99}$ at elevated temperature (figs. 1 and 10), d being very small in this case.

Activation volume measurements, with a minimum value of $70b^3$, confirm that the vacancies are interacting with dislocations in a way that is not exclusively short range (typical values of $5b^3$ occur for short range interactions [20]). If vacancy aggregates rather than single vacancies are considered, stress fields in the lattice would be generated and long range interactions could occur. It is thought [16] that there is an attractive interactions energy between vacancies of 3.5 kcal/mole, resulting in the formation of vacancy aggregates of a size dependent on the temperature and vacancy concentration. The interaction of these obstacles with dislocations will be a dynamic one, the magnitude dependent on hydrogen mobility and dislocation velocity, and will follow the general trends of fig. 10, at the same time being independent of the role of hydrogen diffusion in determining the slip plane.

The only other explanation for vacancy-hardening which occurs to the authors is a change in bonding of the hydride as the hydrogen content is lowered, to a more ionic form with a greater peierls force opposing dislocation motion. This would produce an apparent vacancy-hardening effect, but the observed temperature-dependence and strain-rate dependence of the hardening is then unaccountable.

5. Conclusions

(1) In polycrystalline titanium hydride over the composition range $TiH_{1.58}$ to $TiH_{1.99}$ at all temperatures where plastic strain could be accommodated (generally above 0°C), slip occurs on {111}.

(2) The deformation and fracture characteristics of titanium hydride can be closely related to the hydrogen ion mobility. The hydrogen ion mobility is determined by both temperature and non-stoichiometric defect concentration. A transition from a ductile to a brittle condition over a wide range of composition and test temperature can be correlated with the attainment of a specific value of hydrogen mobility whilst testing at a constant rate of strain.

(3) A consequence of increasing the applied strain rate is an increase, for a particular composition, of the temperature at which the ductile-to-brittle transition occurs.

(4) The yield stress of titanium hydride increases with increasing non-stoichiometric hydrogen vacancy concentration. A more notable feature is the increased temperature-dependence of the yield stress which an increase in the defect concentration produces.

(5) The yield stress is markedly strain-rate sensitive; a two-fold increase in the yield stress being produced by an increase of 400 × in the strain rate.

Acknowledgements

The authors would like to thank K. G. Barraclough, M. H. Loretto and Professor R. E. Smallman for the helpful discussions and comments, and Professor G. V. Raynor for the provision of laboratory facilities. One of us (P.E.I.) would like to thank the University of Birmingham for the provision of a studentship.

References

1. G. G. LIBOWITZ, *J. Nuclear Materials* **2** (1960) 1.
2. *Idem, Adv. Chem. Ser.* **39** (1963) 74.
3. P. E. IRVING and C. J. BEEVERS, *Met. Trans.*, **2** (1971) 613.
4. R. CHANG, *J. Nuclear Materials* **2** (1960) 335.
5. Z. M. AZARKH and P. I. GAVRILOV, *Soviet Phys. Crystallog.* **15** (1970) 231.
6. C. ROY, Ph.D. Thesis, Imperial College, London (1962).
7. K. H. G. ASHBEE, reported by B. Beagley and J. W. Edington, *Brit. J. Appl. Phys.* **14** (1963) 609.
8. J. W. EDINGTON, and M. J. KLEIN, *J. Appl. Phys.* **37** (1966) 3906.
9. R. L. BECK and W. M. MUELLER, "Nuclear Metallurgy" **7** (*Met. Soc. AIME*, 1960) p. 63.
10. K. G. BARRACLOUGH and C. J. BEEVERS, *J. Mater. Sci.* **4** (1969) 518.
11. *Idem, ibid* **4** (1969) 802.
12. *Idem, J. Nuclear Materials* **33** (1969) 296.
13. P. E. IRVING, Ph.D. Thesis, University of Birmingham (1970).
14. N. H. POLAKOWSKI, *J. Iron and Steel Inst.* **163** (1949) 250.
15. G. G. LIBOWITZ and J. G. PACK, Proc. Int. Symp. Conf. on Crystal Growth, Ed. H. S. Peiser (Pergamon Press, 1966) p. 129.
16. T. R. P. GIBB, *Prog. Inorg. Chem.*, **3** (1961) 205.
17. B. STALINSKI, C. K. COOGAN, and H. S. GUTOWSKI, *J. Chem. Phys.* **34** (1961) 1191.
18. G. W. GROVES and A. KELLY, *Phil. Mag.* **8** (1963) 877.
19. T. L. JOHNSTON, R. G. DAVIES, and N. S. STOLOFF, *ibid* **12** (1965) 305.
20. R. J. ARSENAULT, *Acta Metallurgica* **14** (1966) 831.

Received 2 July and accepted 13 July 1971.